Numerical simulation on simplified OCDR without electrical spectrum analyzer

Guangtao Zhu[1], Tomoya Miyamae[1], Kohei Noda[1,2], Heeyoung Lee[3], Kentaro Nakamura[2], and Yosuke Mizuno[1]
[1] Faculty of Engineering, Yokohama National University, Yokohama 240-8501, Japan
[2] Institute of Innovative Research, Tokyo Institute of Technology, Yokohama 226-8503, Japan
[3] College of Engineering, Shibaura Institute of Technology, Tokyo 135-8548, Japan
E-mails: zhu-guangtao-jm@ynu.jp, mizuno-yosuke-rg@ynu.ac.jp

Introduction

In recent years, the application of optical fiber communication technology is experiencing a period of rapid growth, which has created a demand for health monitoring techniques for fiber networks. Among the techniques, optical reflectometry is used to detect positions of poor contact or damage in the fiber by measuring the reflectivity distribution along the fiber under test (FUT).

Widely known optical reflectometry techniques, such as optical time-domain reflectometry (OTDR) [1] and optical frequency-domain reflectometry (OFDR) [2], have the advantages of long measurement range and high spatial resolution, respectively. However, it is sometimes difficult for OTDR and OFDR to perform real-time measurement. To overcome this issue, optical correlation-domain reflectometry (OCDR) has been developed based on the synthesis of optical coherence functions (SOCF), which has the advantages of random accessibility and real-time monitoring [3].

In a standard OCDR configuration, the frequency of the reflected light from the FUT or the reference light is shifted by tens of megahertz by an acoustic optical modulator (AOM) to perform optical heterodyne detection, which can reduce low-frequency noise disturbance [3]. To date, several approaches have been developed to simplify the standard OCDR configuration. For instance, in 2016, AOM-free OCDR was developed by monitoring the foot of reflected peak in the spectrum [4]. Additionally, a simplified OCDR without a reference path was proposed in the same year [5].

In a conventional OCDR configuration, an electric spectrum analyzer (ESA) was used to process the electrical signals. However, the ESA is bulky and high in cost, being an obstacle to system simplicity. In addition, the high-frequency components of the signal are filtered by the built-in low-pass filters in the ESA, leading to reflected peaks with wider bandwidths, which limit the improvement of spatial resolution during high-speed measurement. To tackle this problem, we newly developed an ESA-free OCDR configuration by presenting the experimental setup and results [6]. The results showed its effectiveness on simplifying the conventional system and improving the spatial resolution. However, detailed characterization of the ESA-free OCDR has not been reported yet.

In this work, we numerically simulate the operations of both conventional AOM-free OCDR with an ESA [4] and AOM-free OCDR without an ESA, and compare their performances on distributed reflectivity measurement. The result is highly consistent with the experimental results.

Principle and models

In SOCF-OCDR systems, the optical frequency of the laser output is modulated in a sinusoidal waveform by directly modulating the injection current of the laser. We control the modulation frequency to generate only a single correlation peak (i.e., sensing position) within the range of the FUT. By sweeping the modulation frequency, the position of the correlation peak is scanned along the FUT, and thus the distributed reflectivity measurement can be performed.

The models of both conventional and ESA-free OCDR used in the simulation are shown in Fig. 1. The ESA-free configuration shares an identical AOM-free optical system with the conventional one, while in the ESA-free configuration, the electrical signal converted by the photo detector (PD) with a built-in band-pass filter is directly transmitted to the oscilloscope (OSC) without ESA processing. Therefore, in the conventional OCDR, with the zero-span mode of the ESA, a time-domain signal representing the power at a specific frequency is observed in the OSC. Meanwhile, in the ESA-free OCDR, signal with a wide bandwidth corresponding to the band-pass filter in the PD is observed.

Simulation conditions and results

The model of the FUT used in the simulation is shown in Fig.1. Assume the reflectivity to be 0 except for the position of the reflective surface at 10 m. Distributed reflectivity measurement along the 0–35.8-m section was performed by sweeping the modulation frequency from 2.017 MHz to 2.119 MHz. The number of sampling points was 2,500 at a sampling rate of 250 kHz. The optical wavelength of the laser output was 1,550 nm. In the simulation of the conventional OCDR, the central frequency of the zero-span mode of the ESA was 1 MHz. The video bandwidth (VBW) of the ESA was 30 kHz.

Normalized power distributions of the reflected signal in the conventional and ESA-free configurations are shown in Figs. 2(a), (b). Both configurations effectively detected the reflective surface at 10 m. In the ESA-free OCDR, the reflection peak appeared in both

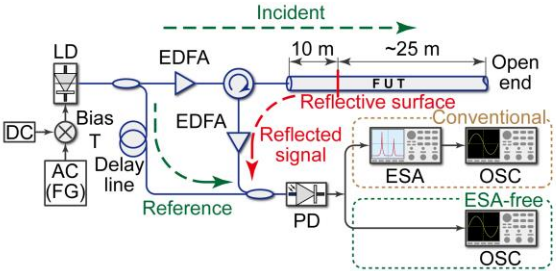

Fig. 1 Models of conventional and ESA-free OCDR configurations used in the simulation. AC: alternating current, DC: direct current, EDFA: erbium-doped fiber amplifier, FG: function generator, LD: laser diode.

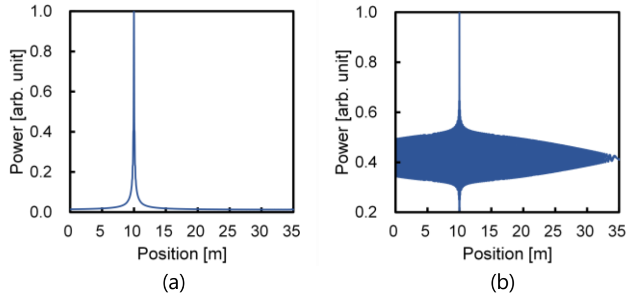

Figs. 2 Normalized power distributions of the reflected signal in (a) conventional OCDR and (b) ESA-free OCDR.

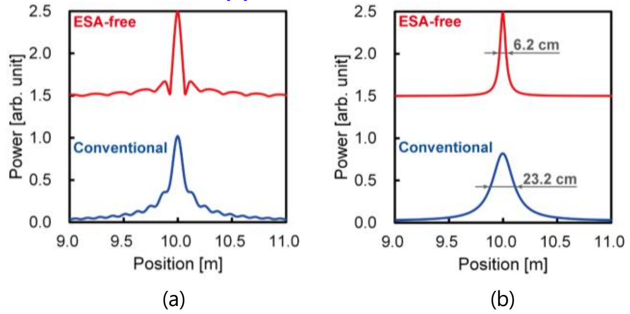

Figs. 3 (a) Normalized power distribution curves of the reflected signal and (b) Lorentzian fitted curves of the distribution curves near the reflective surface, obtained in both conventional and ESA-free OCDR configurations.

positive and negative directions, with a noise floor sandwiched in the middle. Considering that the positive peak was with a higher signal-to-noise ratio (SNR), we zoomed in on the positive side of the data as the result of actual observation.

The normalized power distribution curves of the reflected signal near the reflective surface in the conventional and ESA-free configurations are shown in Figs. 3(a). For conventional OCDR, the result had been filtered by the built-in low pass filter (VBW). For the ESA-free OCDR, the result was obtained by applying the peak-detect function of the OSC on the data near the positive reflection peak and then normalized by setting the maximum power to 1 and power of the noise floor to 0. Subsequently, the power distribution curve of the ESA-free OCDR was elevated by 1.5 overall to be distinguished from that of the conventional OCDR. To quantitatively compare the spatial resolutions of the two configurations, we fitted the distribution curves to Lorentzian functions, as shown in Figs. 3(b). The full width at half maximum (FWHM) of the conventional and ESA-free OCDR are 23.2 cm and 6.2 cm, respectively. The improvement of the spatial resolution by 3.7 times is in good agreement with the previous experimental results [6]. We believe that our simulation will lay a solid foundation for future research on simplified OCDR.

References

[1] M. K. Barnoski, et al., Appl. Opt. **15**, 2112 (1976).
[2] W. Eickhoff, et al., Appl. Phys. Lett. **39**, 693 (1981).
[3] K. Hotate, et al., Meas. Sci. Technol. **15**, 148 (2004).
[4] M. Shizuka, et al., Appl. Phys. Express **9**, 032702 (2016).
[5] M. Shizuka, et al., Appl. Opt. **55**, 3925(2016).
[6] T. Miyamae, et al., JSAP Spring Meeting 2021, 19p-Z05-7.